THE JOURNAL OF PHYSICAL CHEMISTRY A

Article

pubs.acs.org/JPCA

Effect of Bisulfate, Ammonia, and Ammonium on the Clustering of Organic Acids and Sulfuric Acid

Nanna Myllys,[†] Tinja Olenius,[‡] Theo Kurtén,[§] Hanna Vehkamäki,[†] Ilona Riipinen,[‡] and Jonas Elm*[,†]

[†]Department of Physics, University of Helsinki, Helsinki FI-00014, Finland

[‡]Department of Environmental Science and Analytical Chemistry & Bolin Centre for Climate Research, Stockholm University, 106 91 Stockholm, Sweden

[§]Department of Chemistry, University of Helsinki, Helsinki FI-00014, Finland

Supporting Information

ABSTRACT: We investigate the effect of the bisulfate anion HSO_4^-, ammonium cation NH_4^+, and ammonia NH_3 on the clustering of sulfuric acid and pinic acid or 3-methyl-1,2,3-butanetricarboxylic acid (MBTCA). The systems were chosen based on their expected relevance in atmospheric new particle formation. Using quantum chemical methods together with kinetic calculations, we study the ability of these compounds to enhance cluster formation and growth. The cluster structures are obtained and frequencies are calculated using three different DFT functionals (M06-2X, PW91, and ωB97X-D) with the 6-31++G(d,p) basis set. The electronic energies are corrected using an accurate DLPNO−CCSD(T)/def2-QZVPP level of theory. The evaporation rates are evaluated based on the calculated Gibbs free energies. The interaction between the ions and sulfuric acid or carboxylic acid group is strong, and thereby small two-component ionic clusters are found to be very stable against evaporation. The presence of bisulfate stimulates the cluster formation through addition of the sulfuric acid, whereas the presence of ammonium favors the addition of organic acids. Bisulfate and ammonium enhance the first steps of cluster formation; however, at atmospheric conditions further cluster growth is limited due to the weak interaction and fast evaporation of the larger three-component clusters. On the basis of our results it is therefore unlikely that the studied organic acids and sulfuric acid, even together with bisulfate, ammonia, or ammonium can drive new-particle formation via clustering mechanisms. Other mechanisms such as chemical reactions are needed to explain observed new-particle formation events in the presence of oxidized organic compounds resembling the acids studied here.

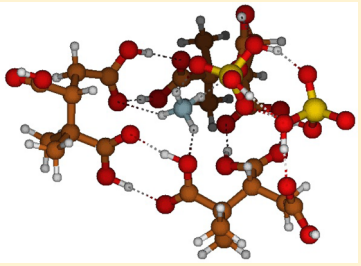

1. INTRODUCTION

New-particle formation via gas-to-particle conversion is a significant source of aerosol particles in the atmosphere.[1,2] Atmospheric aerosols can adversely affect human health and their interactions with clouds constitute one of the largest uncertainties in climate models.[3] Atmospheric new-particle formation is a complex process, which begins when gas-phase molecules collide with each other, and form stable clusters via hydrogen bond formation or acid-to-base proton transfer. Understanding of the exact mechanisms and the participating compounds in various atmospheric locations remains incomplete and there currently is no general theory describing this phenomenon.[2] According to current knowledge, new-particle formation in the present atmosphere often involves sulfuric acid coupled with stabilizing components such as ions, bases, or nonbasic organic compounds.[4−9] It has recently been suggested that low-volatile organic compounds participate in the first steps of new-particle formation,[10,11] but molecular-level explanation and details concerning the involvement of oxidized organic compounds are still missing.[12−14] Specifically, recent laboratory studies have indicated that ions can play a major role in organics-driven particle formation by enhancing the initial molecular cluster formation.[15]

Volatile organic compounds (VOCs) are emitted into atmosphere from both anthropogenic and natural sources. Terpenes, such as α-pinene, constitute a large fraction of biogenic VOCs.[16] In the atmosphere, terpenes are oxidized rapidly in reactions initiated by addition of OH radicals or ozone to a double bond and subsequent reaction with molecular oxygen.[17] The oxidation products cover a wide range of saturation vapor pressures, referred to as volatilities, of which low-volatile and especially extremely low-volatile organic compounds (LVOCs and ELVOCs, respectively) are likely to participate in atmospheric particle formation already at early particle growth stages. The formation of highly oxidized terpene products may occur via autoxidation processes, which involve intramolecular hydrogen-shift reactions and addition of oxygen molecules, and terminate by producing closed-shell species, which are suggested to contain at least one hydroperoxide group.[18,19] There is currently no specific structural information about individual ELVOC species produced via autoxidation from terpenes.[20] Alternatively, terpenes can go through several closed cycles of oxidation reactions.[21] After the

Received: April 27, 2017
Revised: June 6, 2017
Published: June 6, 2017

DOI: 10.1021/acs.jpca.7b03981
J. Phys. Chem. A 2017, 121, 4812−4824

first addition reaction, molecular oxygen addition or rearrangements and termination, the product can be further oxidized by hydrogen abstraction reactions with OH radicals. This process can yield several oxidized compounds, such as pinonaldehyde, pinonic acid, and pinic acid in case of α-pinene.[21,22] Further oxidation of pinonic acid by hydroxyl radicals can lead to the formation of 3-methyl-1,2,3-butanetricarboxylic acid (MBTCA) through complex pathways.[23]

We have previously studied the cluster formation between sulfuric acid and pinic acid or MBTCA and found a favorable molecular interaction between organic acids and sulfuric acid.[24,25] MBTCA forms more stable clusters than pinic acid due to a flexible structure and a larger number of stabilizing hydrogen bonds, and we found clusters consisting of 2−3 MBTCA and 2−3 sulfuric acid molecules to be particularly stable. By cluster kinetics calculations we showed that the growth of the clusters is essentially limited by a weak binding of the largest MBTCA−sulfuric acid clusters, suggesting that pinic acid and MBTCA cannot contribute to the cluster growth when clustering occurs via electrically neutral pathways.

Ions can contribute to new-particle formation and play a stabilizing role to keep condensing species from evaporating. While tropospheric ions have low concentrations compared to neutral species, they are thought to be potentially important in the formation of secondary aerosol particles. Ions are produced continuously throughout the atmosphere due to cosmic rays and as a result of radon decay.[26−28] One of the most common negative ions in the atmosphere is bisulfate, a stable anion with a large electron affinity, and one of the most important atmospheric cations is ammonium. They are believed to be key participants in ion-induced nucleation. In this paper we investigate the stabilizing effect of the bisulfate anion, ammonium cation, and an ammonia molecule on sulfuric acid−pinic acid and sulfuric acid−MBTCA clusters. Stabilizing effect is defined as the ability of these compounds to enhance cluster formation and growth by decreasing the overall evaporation rates of the clusters. Ammonia, for instance, has been shown to significantly stabilize larger particles containing both sulfuric as well as organic acids.[29,30] Furthermore, the presence of ammonium sulfate has been shown the significantly decrease the evaporation of particles containing organic acids[31,32] MBTCA can be seen as a representative ELVOC, while pinic acid, with its relatively weaker binding to clusters, can be seen as a representative LVOC. Figure 1 shows the molecular structures of the pinic acid ($C_9H_{14}O_4$) and MBTCA ($C_8H_{12}O_6$) monomers. The aim of the work is to study if these representative low-volatile species are able to participate in the initial particle formation process together with sulfuric acid via an additional stabilizing compound.

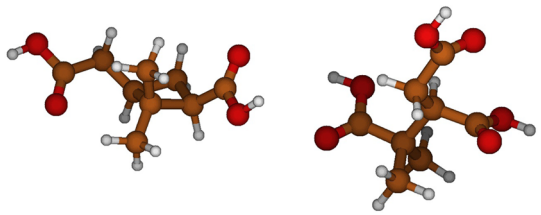

Figure 1. Molecular structure of pinic acid (left) and MBTCA (right). Color coding: brown = carbon, red = oxygen, and white = hydrogen.

2. METHODS

Cluster Structure Sampling. The initial structures for organic acid−sulfuric acid clusters have been taken from our previous studies[24,25] and were used as the starting point for forming the molecular clusters containing also HSO_4^-, NH_4^+, or NH_3. We used the following semiempirically guided technique:[33,34]

1 In each cluster formation step 1000 randomly oriented molecules/ions are randomly distributed around the target molecule/cluster.
2 The structures are initially optimized using the semi-empirical PM6 method.
3 For the converged structures, a single-point M06-2X/6-31+G* energy is calculated.
4 The structures are sorted and characterized by the total energy and dipole moment, and different conformations are identified.
5 Conformations within 15 kcal/mol of the lowest identified conformation are geometry optimized, and frequencies are calculated at the M06-2X/6-31+G* level.
6 Remaining identified conformations within 3 kcal/mol of the lowest conformation are geometry optimized, and frequencies are calculated at the M06-2X/6-31++G** level.

In the case of bisulfate containing clusters, bisulfate is able to move to the center of cluster by proton transfers, thereby forming the minimum energy structure as could be expected. For ammonia and ammonium containing clusters, in addition of sampling them on top of the organic acid-sulfuric acid clusters, we have build larger clusters by sampling different combinations of smaller clusters. By applying this approach we should obtain a good estimate for the global minimum energy conformer.

Cluster Gibbs Free Energies. The cluster binding energies eq 1) and the thermal contributions to the Gibbs free energy (eq 2 are calculated as follows:

$$\Delta E_{\text{binding}} = E_{\text{cluster}} - \sum_i E_{\text{monomer},i} \quad (1)$$

$$\Delta G_{\text{Therm}} = G_{\text{Therm,cluster}} - \sum_i G_{\text{Therm,monomer},i} \quad (2)$$

The cluster Gibbs free binding energies, eq 3, are calculated as the sum of the binding energy and the thermal contribution to the Gibbs free energy. The thermal contribution also contains the vibrational zero point energy.

$$\Delta G_{\text{binding}} = \Delta E_{\text{binding}} + \Delta G_{\text{Therm}} \quad (3)$$

Previous studies have shown that the binding energy is the largest source of error when using only density functional theory to calculate the Gibbs free energy.[12,35] Therefore, we have used a multistep quantum chemical approach to obtain more accurate Gibbs free energies.[36,37] Geometries are optimized and frequencies are calculated using three density functionals, M06-2X,[38] PW91,[39] and ωB97X-D,[40] with the 6-31++G** basis set.[41] These functionals have been shown to perform well in describing atmospheric molecular clusters involving sulfuric acid.[42−44] In addition, we have performed benchmark calculations to further confirm that 6-31++G** basis set is indeed sufficient to obtain reliable molecular structure and vibrational frequencies (see Supporting Information). Thermochemical parameters are calculated using the

DOI: 10.1021/acs.jpca.7b03981
J. Phys. Chem. A 2017, 121, 4812−4824

rigid rotor-harmonic oscillator approximation (RRHO), and unless otherwise mentioned, at 298.15 K and reference pressure 1 atm. The RRHO approximations can be a source of errors in atmospheric cluster formation calculations. The effect of vibrational anharmonicity has previously been studied for water clusters using vibrational second order perturbation theory (VPT2) and derived vibrational frequency scale factors, where it was found that the formation free energy was lowered approximately 0.4 kcal/mol per water molecule in a 10-water cluster.[45] For more rigid clusters consisting of four sulfuric acid molecules and four bases the lowering in free energy has been found to be below 2 kcal/mol.[35] Low lying vibrational frequencies can also be a source of errors in free energy calculations. By treating low vibrational frequencies as rotations instead of vibrations, known as the quasi-harmonic approximation,[46] the free energy was found to be up to 7 kcal/mol higher compared to the harmonic oscillator approximation.[35] Hence the errors arising from the harmonic oscillator approximation thereby show contributions in opposite directions and a partial error cancellation can be assumed.

All density functional theory calculations were run using Gaussian09.[47] Electronic energy corrections were performed using a domain-based local pair natural orbital coupled cluster, DLPNO−CCSD(T),[48,49] with the def2-QZVPP basis set[50] using ORCA version 3.0.3.[51] DLPNO−CCSD(T) yields results close to the quantum chemical gold standard, CCSD(T), with significantly reduced computational cost. Our earlier studies have shown that DLPNO−CCSD(T) yields binding energies with lower stability than canonical coupled cluster methods, and therefore it can be used as a lower bound for the "true" cluster binding energies.[12] As basis set incompleteness and basis set superposition errors can be a large sources of error in correlated binding energy calculations, we have studied the basis set convergence of the DLPNO−CCSD(T) method, and found that the def2-QZVPP basis set offers good accuracy with low computational costs and is thus a sufficient basis set for large molecular clusters (see Supporting Information). Because of the large system size, up to 105 atoms (6305 basis functions), we have performed all DLPNO calculations using local trafo (LT) type 3 to reduce memory requirements. We have shown that using this LT type does not yield errors for the binding energies (see Supporting Information).

Cluster Kinetics. For a cluster to be stable at given conditions requires that its collision rate with vapor molecules (or clusters) is equal to or higher than its evaporation rate. We have performed kinetics calculations for both neutral and ionic sulfuric acid-organic acid clusters to look further into the stability of the clusters. According to the law of mass balance, for a cluster $(i + j)$ formed from isolated monomers i and j as

$$i + j \rightleftharpoons (i + j) \tag{R1}$$

the equilibrium constant K can be written as

$$K = \frac{C_{i+j}^{eq}}{(C_i^{eq})(C_j^{eq})} = \frac{k_B T}{p_{ref}} \exp\left(-\frac{\Delta G}{k_B T}\right) \tag{4}$$

where C_i^{eq} is the equilibrium concentration of compound i, k_B is the Boltzmann constant, T is the temperature, ΔG is the Gibbs free energy of reaction R1, and p_{ref} is the reference pressure at which ΔG is computed. At equilibrium (and assuming detailed balance conditions) cluster formation must be equal to cluster destruction, i.e., evaporation, as

$$\gamma_{(i,j)} C_{i+j}^{eq} = \beta_{i,j} C_i^{eq} C_j^{eq} \tag{5}$$

where $\gamma_{(i,j)}$ is the evaporation rate and $\beta_{i,j}$ is the collision rate.

The collision coefficients for neutral−neutral collisions are calculated from kinetic gas theory[52] as

$$\beta_{i,j} = \left(\frac{3}{4\pi}\right)^{1/6} \left[6 k_B T \left(\frac{1}{m_i} + \frac{1}{m_j}\right)\right]^{1/2} (V_i^{1/3} + V_j^{1/3})^2 \tag{6}$$

where m_i and V_i are the mass and volume of cluster i, respectively. The volumes are calculated using bulk liquid densities assuming spherical clusters and ideal mixing. For density of sulfuric acid we used $\rho = 1830 \frac{kg}{m^3}$ and for pinic acid $\rho = 1200 \frac{kg}{m^3}$. As the density of MBTCA is unknown, we have used $\rho = 1400 \frac{kg}{m^3}$, which is similar to other $C_8H_{12}O_6$ compounds.

In the collisions between ions and neutral molecules or clusters, the collision cross section is larger than would be predicted from the physical dimensions of the colliding systems due to their long-range attraction.[53] For the neutral-ion collision coefficients we have applied the approach by Su and Chesnavich,[54] who performed trajectory simulations of collisions between a point charge and a rigidly rotating molecule. They found that the collision frequency is dependent on three reduced parameters:

$$\beta_{i,j}^L = q_i \left(\frac{1}{m_i} + \frac{1}{m_j}\right)^{1/2} \left(\frac{\pi \alpha_j}{\epsilon_0}\right)^{1/2}$$

$$I^* = \frac{\mu_j I}{\alpha_j q_i} \left(\frac{1}{m_i} + \frac{1}{m_j}\right)$$

$$x = \frac{\mu_j}{(8\pi\epsilon_0 \alpha_j k_B T)^{1/2}}$$

Here q_i is the charge of the ion, α_j, μ_j, and I are the polarizability, dipole moment, and moment of inertia of the neutral molecule, respectively, and ϵ_0 is the vacuum permittivity. At low values of I^*, i.e., when $I^* < \frac{0.7 + x^2}{2 + 0.6x}$, the collision rate was observed to be independent of I^*, and a fit to the simulated data produced the parametrization

$$\beta_{i,j} = \begin{cases} \beta_{i,j}^L (0.4767x + 0.6200), & x \geq 2 \\ \beta_{i,j}^L \left(\frac{(x + 0.5090)^2}{10.526} + 0.9754\right), & x < 2 \end{cases} \tag{7}$$

The parametrization has been compared with experimental collision rates and was found to give a good correspondence.[53]

The evaporation rates of the clusters are obtained from the Gibbs free energies by assuming detailed balance as in eq 5:[55]

$$\gamma_{(i,j)\rightarrow i,j} = \beta_{i,j} \frac{p_{ref}}{k_B T} \exp\left(\frac{\Delta G_{i+j} - \Delta G_i - \Delta G_j}{k_B T}\right) \tag{8}$$

where ΔG values are the formation free energies of the evaporating cluster and its products at temperature T and pressure p_{ref}. It should be noted that the reference pressure p_{ref} will cancel out from the evaporation rate.

DOI: 10.1021/acs.jpca.7b03981
J. Phys. Chem. A 2017, 121, 4812−4824

Table 1. Gibbs Free Binding Energies (kcal/mol) for Pinic Acid Clusters Calculated at the DLPNO//DFT Level of Theory at 298.15 K and 1 atm[a]

			X = bisulfate	X = ammonia	X = ammonium
		1P1X	−12.1 (0.6)	0.2 (0.5)	−25.9 (0.5)
1P1A	−5.7 (0.1)	1P1A1X	−30.9 (1.2)	−10.6 (0.6)	−29.1 (0.7)
1P2A	−10.5 (0.3)	1P2A1X	−46.3 (0.8)	−21.2 (0.5)	−35.4 (0.9)
2P	0.0 (1.2)	2P1X	−18.6 (0.5)	3.0 (1.6)	−33.6 (0.2)
2P1A	−9.9 (1.2)	2P1A1X	−33.8 (0.3)	−13.4 (0.8)	−35.5 (1.4)
2P2A	−16.8 (1.3)	2P2A1X	−39.5 (1.8)	−22.2 (0.2)	−40.9 (0.5)
		1A1X	−32.0 (0.3)	−4.8 (0.2)	−11.9 (0.6)
2A	−5.2 (0.1)	2A1X	−48.1 (0.6)	−8.9 (0.3)	−22.6 (0.5)

[a]The standard deviations are given in parentheses. Abbreviations: P = pinic acid and A = sulfuric acid.

3. RESULTS AND DISCUSSION

Formation of Pinic Acid Clusters. The Gibbs free energies are calculated for clusters up to $(C_9H_{14}O_4)_2(H_2SO_4)_2(X)_1$, where X = HSO_4^-, NH_3, or NH_4^+. For simplicity, we will refer to pinic acid as P, H_2SO_4 as A, HSO_4^- as B, NH_3 as N, and NH_4^+ as C. The initial structures for the pinic acid-sulfuric acid clusters have taken from ref 25 and reoptimized at the M06-2X/6-31++G** level of theory. Bisulfate, ammonia, and ammonium are added to the M06-2X clusters using the sampling technique explained above. For the lowest energy structures, the calculations are performed with the three density functionals M06-2X, PW91, and ωB97X-D using a 6-31++G** basis set and the single point energies (SPEs) are calculated on top of the DFT structures at the DLPNO−CCSD(T)/def2-QZVPP level of theory. The final Gibbs free energies are given as averages of the values obtained with the different functionals. To estimate the sensitivity of the calculated free energy to the functional used in obtaining the geometry and vibrational frequencies, we report the scatter in the free energy as the standard deviation σ. Table 1 shows the Gibbs free binding energies at 298.15 K and 1 atm, corresponding to conditions in the lower troposphere.

The presence of ammonia yields Gibbs free binding energies several kcal/mol more negative compared to the bimolecular sulfuric acid-pinic acid clusters. The only exception is the pinic acid dimer, where the ammonia destabilizes the cluster structure. The presence of bisulfate or ammonium makes the Gibbs free binding energies about 20 kcal/mol more negative compared to the two-component sulfuric acid-pinic acid clusters. It should be noted that the interaction with bisulfate and sulfuric acid is so strong that a large part of apparent stabilizing effect is originating from the interaction between bisulfate and sulfuric acid. The presence of bisulfate or ammonium stabilizes the pinic acid dimer structure compared to the bimolecular dimer by 18.6 and 33.6 kcal/mol, respectively. Both bisulfate and ammonium form three hydrogen bonds with the carboxylic acid groups, whereas ammonia forms only two (see Figure 2).

Figure 3 shows the reaction Gibbs free energy diagrams for the pinic acid clusters at 298.15 K. The digram shows whether a given cluster addition reaction is favorable (green, $\Delta G < -10$ kcal/mol) or not (red, $\Delta G > -5$ kcal/mol). For bimolecular pinic acid-sulfuric acid clusters, none of the reaction steps−even the first ones−are thermodynamically highly favorable. The interaction between bisulfate and sulfuric acid is very strong, and thus the addition of pinic acid to the 1A1B or 2A1B clusters is thermodynamically unfavorable. Bisulfate containing clusters can more likely grow via the 1P1B cluster, which is stabilized by two hydrogen bonds with bisulfate and carboxylic acid groups (see Figure 4). The addition of a second pinic acid molecule to the 1P1B cluster is favorable by −6.5 kcal/mol. The addition of sulfuric acid to the 2P1B cluster is highly favorable (−15.2 kcal/mol) and the addition of a second sulfuric acid molecule is slightly favorable (−5.7 kcal/mol). However, the Gibbs free binding energy of the 2P2A1B cluster is much less negative than the Gibbs free binding energy of 2A1B, thus even if the 2P2A1B cluster is formed it will most likely evaporate rapidly.

The interaction between ammonia and pinic acid or sulfuric acid is relatively weak, and none of the formation routes are

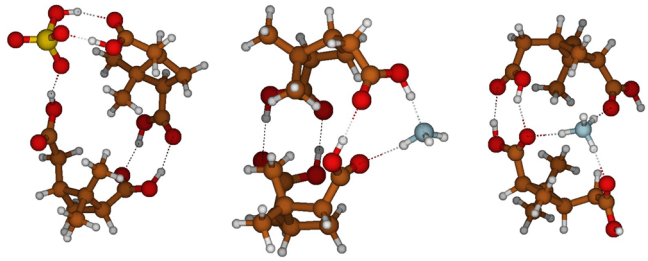

Figure 2. Pinic acid dimer with bisulfate (left), ammonia (middle), and ammonium (right).

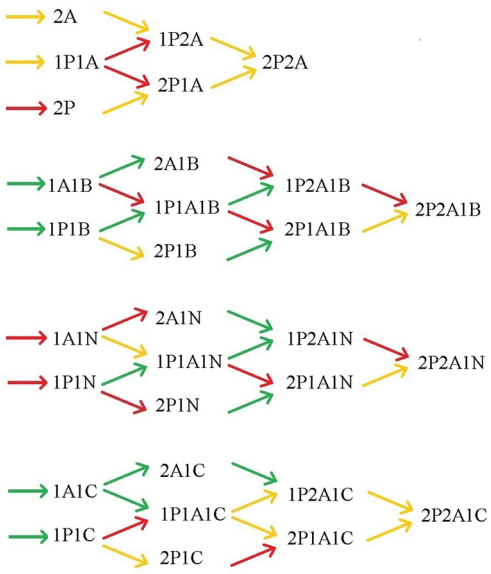

Figure 3. Gibbs free energy diagrams for pinic acid clusters at 298.15 K and 1 atm calculated at DLPNO//DFT level. Color coding: red > −5 kcal/mol, yellow −5 to −10 kcal/mol, and green < −10 kcal/mol. Abbreviations: P = pinic acid, A = sulfuric acid, B = bisulfate, N = ammonia, and C = ammonium.

DOI: 10.1021/acs.jpca.7b03981
J. Phys. Chem. A 2017, 121, 4812−4824

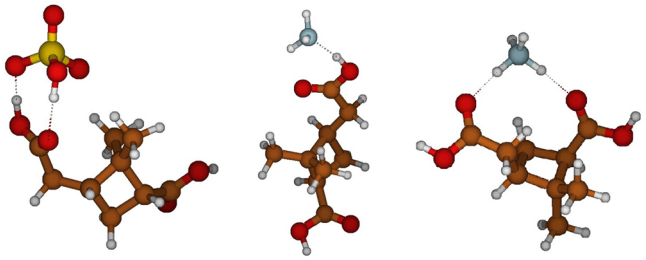

Figure 4. Pinic acid interaction with bisulfate (left), ammonia (middle), and ammonium (right).

thermodynamically favorable. Only one hydrogen bond is formed between ammonia and pinic acid as can see from Figure 4. There is no proton transfer occurring in the 1P1A1N cluster, and the addition of a second pinic acid or sulfuric acid is needed to facilitate a proton transfer from sulfuric acid to ammonia (see Figure 5). Ammonium interacts strongly with pinic acid

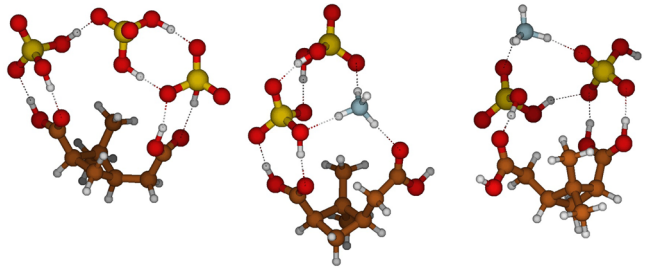

Figure 5. Clusters containing pinic acid and two sulfuric acid with bisulfate (left), ammonia (middle), and ammonium (right).

and sulfuric acid by forming two hydrogen bonds. The hydrogen bonds with sulfuric acid are relatively weak as the hydrogen bond angles are 140°, whereas pinic acid is able to bend and form stronger, nearly linear hydrogen bonds as illustrated in Figure 4. However, cluster growth via the 1P1C cluster is unlikely due to the unfavorable reaction routes. The growth of ammonium containing clusters can more likely be initiated by forming the 1A1C cluster, for which the addition of pinic acid or a second sulfuric acid is thermodynamically favorable. The 1P1A1C cluster can grow either by addition of a second pinic acid or sulfuric acid molecule, both with reaction free energies of −6 kcal/mol, and formation of the 2P2A1C cluster is also thermodynamically slightly favorable (−5 kcal/mol). The growth may also occur by formation of the 2A1C cluster, for which the addition of pinic acid has a favorable Gibbs free energy. There is a proton transfer from sulfuric acid to pinic acid in the 1P2A1C cluster as illustrated in Figure 5. Similar base-like behavior is also found for phosphoric acid when it interacts with two sulfuric acid molecules.[56]

The standard Gibbs free energies ΔG_{ref}, calculated at the reference pressure p_{ref}, do not include the effect of the vapor-phase concentrations of the clustering species. From the law of mass action, the actual, vapor-concentration-dependent Gibbs free energies of the clusters at given vapor concentrations C_i can be obtained as

$$\Delta G_{actual}(C_1, C_2, ..., C_n) = \Delta G_{ref} - k_B T \sum_{i=1}^{n} N_i \ln\left(\frac{C_i}{C_{ref}}\right) \quad (9)$$

where the summation goes over all compounds i in the cluster, and $C_{ref} = p_{ref}/(k_B T)$. To examine the clustering thermodynamics at atmospheric conditions, we calculated the actual free energies at atmospherically relevant concentrations of sulfuric acid and pinic acid. For simplicity, the concentration of the third compound (HSO_4^-, NH_3, or NH_4^+) was not considered in the conversion of eq 9, since it only adds a constant term to all ΔG_{actual} values of a given three-component system, and does not affect the relative free energies on the H_2SO_4−pinic acid grid.

Figure 6 shows the actual DLPNO//DFT Gibbs free energy surfaces for pinic acid clusters at 273 K, when [H_2SO_4]= about 1 ppt (10^7 molecules/cm^3) and [pinic acid] = 10 ppt (about 10^8 molecules/cm^3). A temperature of 273 K was chosen as it corresponds to spring-time new particle formation events observed in the field, as well as experiments simulating real atmospheric conditions such as in the CLOUD chamber. In the case of two-component sulfuric acid-pinic acid clusters, every addition of either pinic acid or sulfuric acid leads to a higher formation free energy. The presence of bisulfate enhances the cluster affinity toward sulfuric acid; i.e., the addition of sulfuric acid to a cluster containing bisulfate is always lower than that to the corresponding clusters without bisulfate, except in the case of 2P1A1B. In ammonia containing clusters, there is only one step yielding to slightly lower free energy, the addition of sulfuric acid to the 2P1N cluster. For other clusters in this system, however, there is no clearly favorable growth direction, i.e., the addition of either sulfuric acid or pinic acid, that would lead to a lower formation free energy. Following the lowest free energy path, the cluster formation begins with the interaction between sulfuric acid and ammonia, and the following step is the addition of pinic acid. The addition of sulfuric acid to the 1P1A1N cluster has a lower free energy barrier than adding pinic acid. The presence of ammonium favors the addition of pinic acid compared to the addition of sulfuric acid, which might be due to the strong interaction between ammonium and carbonyl groups. The addition of the first pinic acid molecule yields a lower formation free energy, but the addition of the second pinic acid leads to a higher formation free energy. The lowest free energy path passes through the formation of the 2P1C cluster. No critical cluster exists within any of the studied systems at the given conditions. At the same conditions, based on the average DFT Gibbs free energies (the Gibbs free energies without coupled cluster energy corrections), the qualitative trend of free energy surfaces is exactly the same as with DLPNO corrections, except the addition of pinic acid to the 1P2A1C cluster, which leads to a lower formation free energy (see Supporting Information).

Figure 7 shows the overall evaporation rates $\sum\gamma$ at 273 K based on the DLPNO//DFT Gibbs free energies. All evaporation rates are found to be high, with the exception of the sulfuric acid and bisulfate containing clusters and the pinic acid-ammonium ion cluster. The free energy barriers are reduced at lower temperature and the reduction of temperature to 243 K yields approximately 3 orders of magnitude lower evaporation rates (see Supporting Information). The evaporation frequencies remain, however, high compared to molecular collision frequencies $\beta_{i,\,cluster} \times C_i$ at typical atmospheric vapor concentrations C_i, which are of the order ~10^{-4} to 10^{-2} s^{-1}. Interestingly, a relatively low evaporation rate is predicted for the 1P2A1N cluster. However, even at a low temperature, the overall evaporation rates are significant, and thus the growth of pinic acid containing clusters is very

DOI: 10.1021/acs.jpca.7b03981
J. Phys. Chem. A 2017, 121, 4812−4824

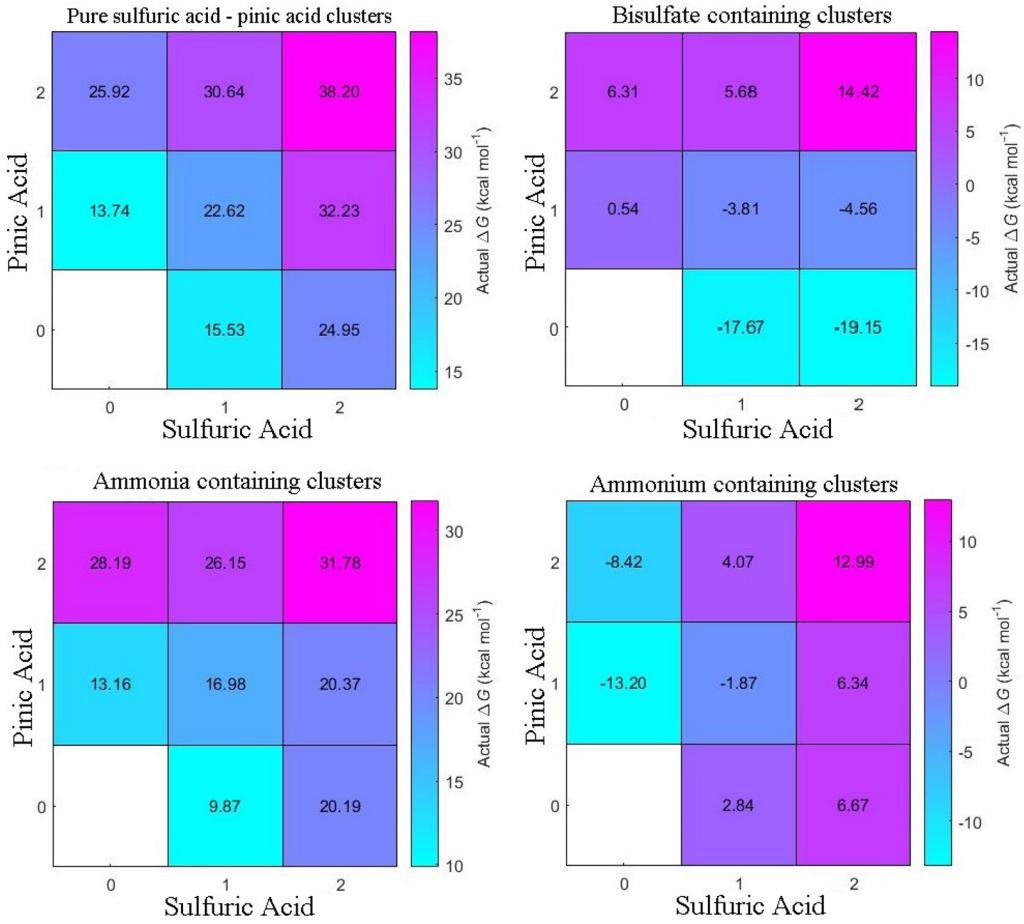

Figure 6. Actual Gibbs free energies (kcal/mol) for pinic acid clusters at 273 K based on DLPNO//DFT free energies. $[H_2SO_4] = 10^7$ molecules/cm^3 and [pinic acid] = 10 ppt. Note the different color scale of the Gibbs free energies.

unlikely, which is consistent with our previous study of the neutral sulfuric acid-pinic acid clusters.[25] We have also calculated the evaporation rates at 298 K, which further confirms that none of the three-component clusters are stable against evaporation at atmospheric conditions (see Supporting Information).

The DLPNO−CCSD(T) method has been observed to underbind compared to canonical coupled cluster methods, and thus our results can be used as a lower bound for binding energies.[37] The DFT functionals predict higher cluster stability than DLPNO, and DFT often overbinds compared to the canonical coupled cluster binding energies, but the overbinding is not consistent. To get an estimate of the lower bound for the evaporation rates and to eliminate random DFT errors, we have calculated the overall evaporation rates at 273 K based on the average DFT Gibbs free energies (see Supporting Information). In most cases, the qualitative prediction of DFT is similar to DLPNO; for example, both predict a low evaporation rate for the 1P2A1N cluster. The only significant qualitative difference is the 2P2A1C cluster, for which DLPNO predicts an evaporation rate similar to the surrounding clusters, but DFT predicts a several orders of magnitude lower evaporation rate.

Often the evaporation rates of two-component sulfuric acid−pinic acid clusters are lower than those of the corresponding bisulfate, ammonia, or ammonium containing clusters. In the case of bisulfate, the interaction between sulfuric acid and bisulfate is significantly stronger than any other interaction, and therefore all clusters containing both sulfuric acid and bisulfate are evaporating toward 1A1B or 2A1B clusters. For example, the evaporation rates (at 273 K based on the DLPNO//DFT energies) for different 1P1A1B evaporation pathways are

$$1P1A1B \rightarrow 1P1B + 1A \quad \gamma_2 = 7 \times 10^{-6}\ s^{-1} \qquad (R2)$$

$$1P1A1B \rightarrow 1A1B + 1P \quad \gamma_3 = 7 \times 10^{10}\ s^{-1} \qquad (R3)$$

$$1P1A1B \rightarrow 1B + 1P1A \quad \gamma_4 = 7 \times 10^{-11}\ s^{-1} \qquad (R4)$$

indicating that the total evaporation is primarily caused by the R3 pathway since its rate is 16 orders of magnitude higher than that of R2. However, the presence of bisulfate in the 2P1B cluster enhances stability against evaporation compared to the homomolecular pinic acid dimer. The main evaporation route for the 2P1B cluster is 1P1B + 1P.

The presence of ammonia increases evaporation rates of pinic acid-sulfuric acid clusters by 1−5 orders of magnitude, except in the case of 1P2A1N for which the evaporation rate is 4 orders of magnitude lower than for the 1P2A cluster. For the 1P2A1N cluster, the main evaporation pathways are 1P1A1N + 1A and 1P1A + 1A1N, both with nearly equal evaporation rates. The evaporation rate of 2P1N is 4 orders of magnitude higher than that of the homomolecular pinic acid dimer, and the evaporation rate for 2P + 1N is ten times higher than for the 1P1N + 1P pathway.

The presence of ammonium ion increases evaporation of pinic acid−sulfuric acid clusters due to the strong interaction

DOI: 10.1021/acs.jpca.7b03981
J. Phys. Chem. A 2017, 121, 4812−4824

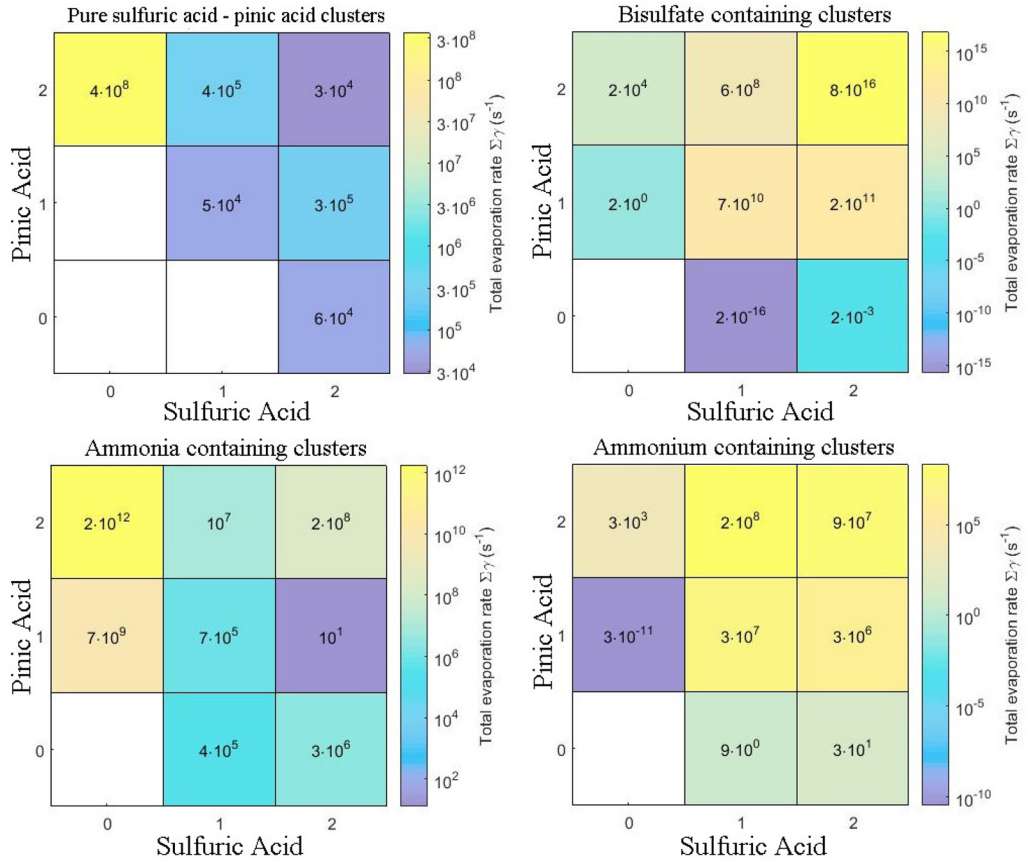

Figure 7. Overall evaporation rates ($\sum\gamma$ (s^{-1})) for pinic acid clusters at 273 K based on DLPNO//DFT free energies. Note the different color scale of the total evaporation rates.

Table 2. Gibbs Free Binding Energies (kcal/mol) for MBTCA Clusters Calculated Using DLPNO//DFT Level of Theory at 298.15 K and 1 atm[a]

			X = bisulfate	X = ammonia	X = ammonium
		1M1X	−20.8 (0.4)	−0.3 (0.5)	−23.5 (0.2)
1M1A	−6.2 (0.2)	1M1A1X	−35.0 (0.2)	−8.9 (0.6)	−28.0 (0.3)
1M2A	−8.5 (0.3)	1M2A1X	−42.7 (0.2)	−16.6 (0.4)	−34.7 (1.3)
1M3A	−12.3 (0.9)	1M3A1X	−51.2 (2.5)	−24.7 (0.1)	−39.5 (1.1)
1M4A	−19.1 (1.7)	1M4A1X	−60.6 (1.3)	−30.4 (0.9)	−39.0 (3.0)
2M	−1.2 (0.8)	2M1X	−24.6 (1.0)	−2.3 (1.3)	−35.6 (0.5)
2M1A	−10.2 (0.8)	2M1A1X	−39.9 (1.1)	−12.1 (1.1)	−28.7 (0.9)
2M2A	−20.1 (1.1)	2M2A1X	−50.4 (0.1)	−24.3 (0.7)	−49.6 (0.8)
2M3A	−30.7 (0.8)	2M3A1X	−56.5 (3.3)	−35.8 (0.3)	−57.0 (0.6)
2M4A	−32.8 (2.5)	2M4A1X	−62.5 (1.9)	−43.4 (1.8)	−55.6 (1.6)
3M1A	−15.0 (0.5)	3M1A1X	−37.5 (0.8)	−22.3 (1.5)	−41.7 (0.2)
3M2A	−25.7 (1.1)	3M2A1X	−55.1 (0.3)	−38.7 (1.8)	−54.7 (1.0)
3M3A	−29.1 (2.9)	3M3A1X	−56.3 (2.1)	−41.0 (1.3)	−62.8 (1.5)
		1A1X	−32.0 (0.3)	−4.8 (0.2)	−11.9 (0.6)
2A	−5.2 (0.1)	2A1X	−48.1 (0.6)	−8.9 (0.3)	−22.6 (0.5)

[a]The standard deviations are given in parentheses. Abbreviations: M = MBTCA and A = sulfuric acid.

between pinic acid and ammonium. The main evaporation products are 1P1C and 2P1C. For example, the evaporation rates (at 273 K based on DLPNO//DFT energies) for different 1P1A1C evaporation pathways are

$$1P1A1C \rightarrow 1P1C + 1A \quad \gamma_5 = 3 \times 10^7\ s^{-1} \qquad (R5)$$

$$1P1A1C \rightarrow 1A1C + 1P \quad \gamma_6 = 1 \times 10^{-4}\ s^{-1} \qquad (R6)$$

$$1P1A1C \rightarrow 1C + 1P1A \quad \gamma_7 = 5 \times 10^{-9}\ s^{-1} \qquad (R7)$$

indicating that reaction R5 determines the total evaporation rate because of the strong binding between ammonium and carboxylic acid groups. As there is a strong interaction between ammonium and pinic acid, the evaporation rate of 2P1C is 4 orders of magnitude lower than that of 2P, and the main evaporation products are 1P1C + 1P.

The main evaporation routes of 2P2A1C are

DOI: 10.1021/acs.jpca.7b03981
J. Phys. Chem. A 2017, 121, 4812−4824

$$2P2A1C \rightarrow 2P1C + 2A \quad (R8)$$

$$2P2A1C \rightarrow 2P1A1C + 1A \quad (R9)$$

The DLPNO//DFT level predicts that the rate for reaction R8 is 330 times higher than that of reaction R9, whereas according to the DFT calculations, the evaporation rates for these reactions are of the same order.

Formation of MBTCA Clusters. We have calculated the Gibbs free energies for clusters up to $(C_8H_{12}O_6)_3(H_2SO_4)_3(X)_1$, where X = HSO_4^-, NH_3, or NH_4^+. For simplicity we will refer to MBTCA as M. The initial structures for the MBTCA−sulfuric acid clusters have been taken from ref 24, and the HSO_4^-, NH_3, and NH_4^+ are added to the clusters using the same sampling technique as described previously. The calculations for the minimum energy structures are performed using DLPNO−CCSD(T)/def2-QZVPP//DFT/6-31++G** level of theory. Table 2 shows the Gibbs free binding energies and the scatter in the free energy as 1 standard deviation.

Ammonia decreases the formation Gibbs free energies of MBTCA-sulfuric acid clusters by several kcal/mol in all cases. Contrary to the pinic acid dimer, ammonia is able to stabilize the MBTCA dimer structure by forming a hydrogen bond with the nonbonding carboxylic acid group (see Figure 8). Bisulfate and ammonium stabilize the MBTCA dimer structure by 23.4 and 34.4 kcal/mol, respectively.

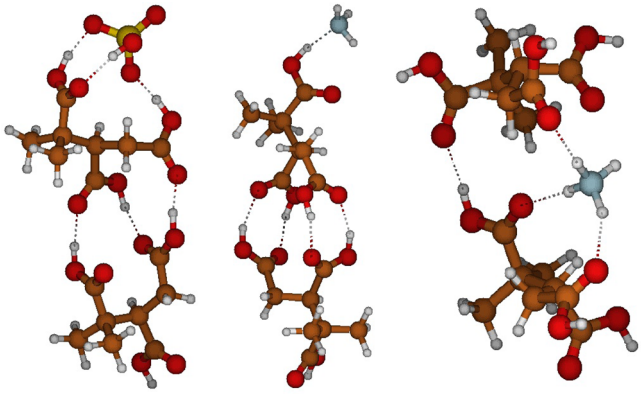

Figure 8. MBTCA dimer with bisulfate (left), ammonia (middle), and ammonium (right).

Bisulfate and ammonium ions bind strongly with MBTCA by hydrogen-bond formation, but the interaction between ammonia and the carboxylic acid group is weak (see Figure 9). Both bisulfate and ammonia decrease the formation Gibbs free energies by 20−40 kcal/mol compared to the bimolecular

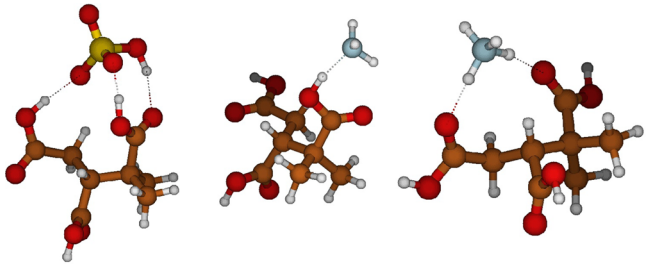

Figure 9. MBTCA monomer binding with bisulfate (left), ammonia (middle), and ammonium (right).

MBTCA−sulfuric acid clusters. It should be kept in mind that the interaction with sulfuric acid and ions is strong, especially in the case of bisulfate, and thus the low Gibbs free energy values are mainly originating from the binding of sulfuric acid molecules to the ions.

Figure 10 shows the reaction Gibbs free energy diagrams for the MBTCA clusters. Similarly to the pinic acid clusters, the

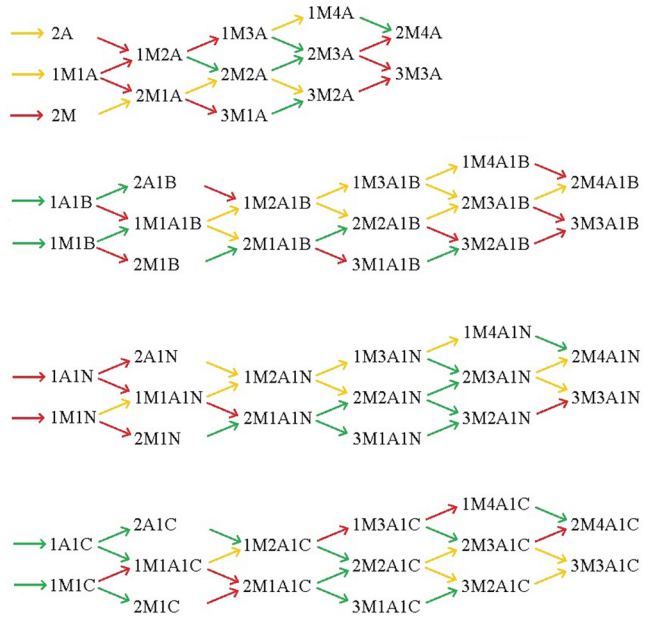

Figure 10. Gibbs free energy diagrams for MBTCA clusters at 298.15 K and 1 atm calculated at the DLPNO//DFT level. Color coding: red > −5 kcal/mol, yellow −5 to −10 kcal/mol, and green < −10 kcal/mol. Abbreviations: M = MBTCA, A = sulfuric acid, B = bisulfate, N = ammonia, and C = ammonium.

first steps of bimolecular MBTCA-sulfuric acid cluster formation are not thermodynamically favorable, and the only highly favorable additions of MBTCA are to the 1M2A, 1M3A, and 1M4A clusters, where sulfuric acid molecules are able to bridge between two MBTCA molecules. The presence of ammonia enhances the formation of larger clusters, but the first steps are still unfavorable. Both bisulfate and ammonium ions are able to bind strongly with sulfuric acid and MBTCA, and therefore the initial clustering steps are highly favorable in these systems. In the case of bisulfate, the addition of the first or second sulfuric acid molecule is a highly favorable process, and the addition of the third or fourth sulfuric acids is less favorable. The addition of MBTCA is not highly favorable for any cluster, which implies that bisulfate and sulfuric acid are clustering with each other independently of whether or not MBTCA is present. Ammonium seems to be a better compound than bisulfate to enhance the growth of MBTCA clusters. In the studied system, the growth of ammonium-containing clusters begins most likely by forming the 2A1C cluster, with subsequent addition of two MBTCA molecules, all steps being thermodynamically highly favorable. The 2M2A1C cluster can grow either by addition of a third MBTCA or sulfuric acid molecule, with reaction free energies of −5 and −7 kcal/mol, respectively. The formation of the 3M3A1C cluster is also thermodynamically slightly favorable. The growth may also occur via the 1M1A1C cluster, for which the addition of a second sulfuric acid is favorable with a reaction free energy of −7 kcal/mol.

DOI: 10.1021/acs.jpca.7b03981
J. Phys. Chem. A 2017, 121, 4812−4824

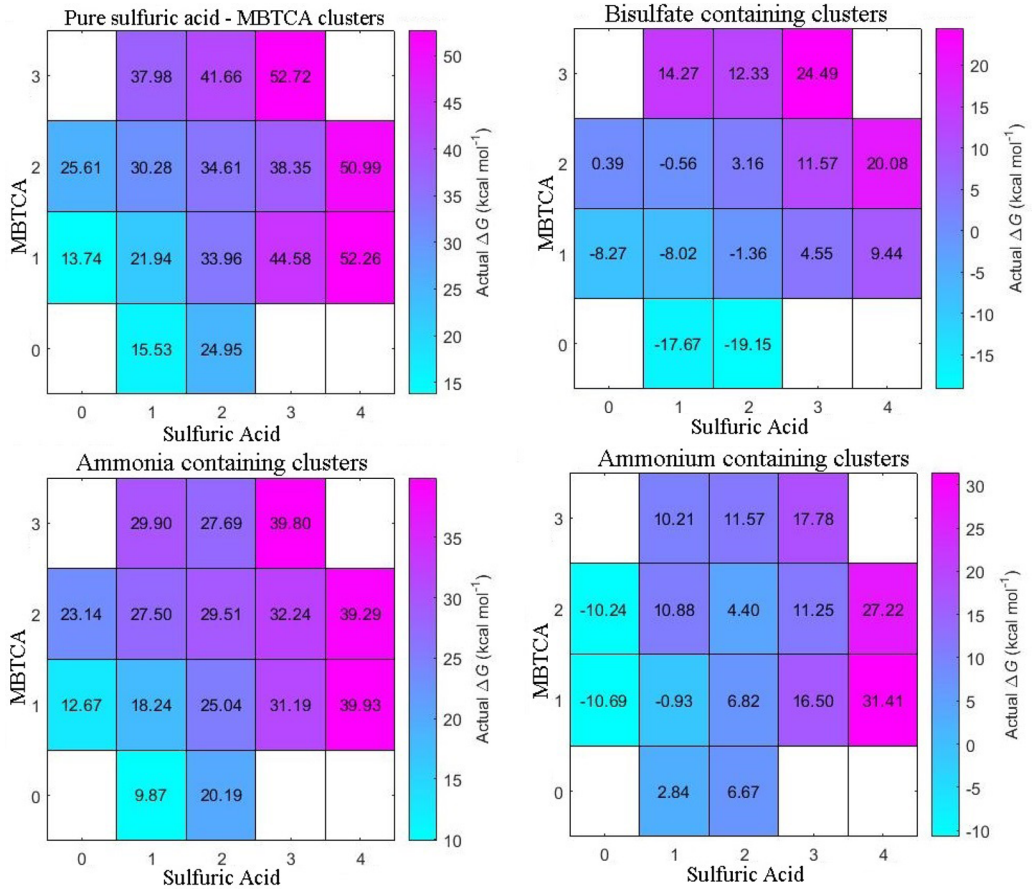

Figure 11. Actual Gibbs free energies (kcal/mol) for MBTCA clusters at 273 K based on DLPNO//DFT free energies. $[H_2SO_4] = 10^7$ molecules/cm^3 and [MBTCA] = 10 ppt. Note the different color scale of the Gibbs free energies.

Figure 11 presents the actual Gibbs free energy surfaces of MBTCA clusters at 273 K, $[H_2SO_4] = 10^7$ molecules/cm^3 and [MBTCA] = 10 ppt. There is no favorable growth direction on the bimolecular MBTCA-sulfuric acid cluster grid, since every addition of sulfuric acid or MBTCA molecule leads to a higher formation free energy. In the case of bisulfate clusters, the formation of 1M1B, 1A1B, and 2A1B clusters yields a lower formation free energy. Addition of sulfuric acid to the 3M1A cluster leads to a lower actual Gibbs free energy. However, other addition steps lead to a higher free energy. In ammonia-containing clusters, the formation of 3M2A1N cluster yields a lower free energy from both direction, i.e., the addition of sulfuric acid to 3M1A1N or the addition of MBTCA to 2M2A1N. All other formation steps lead to a higher formation free energy. Following the lowest free energy path, the clustering begins with the interaction of sulfuric acid and ammonia, and continues by an addition of MBTCA. The 1M1A1N cluster grows by an addition of sulfuric acid, followed by two consecutive additions of MBTCA molecules. In the presence of ammonium, there are several addition steps which yield a lower formation free energy. The actual free energy surface suggests that the clustering may begin with the collision between MBTCA and ammonium, followed by addition of a second MBTCA molecule. The 2M1C cluster grows by three sequential additions of sulfuric acid, followed by a third MBTCA. It must be noted, however, that the free energy surface alone does not determine the most likely growth pathways: thermodynamically favorable paths may not be major growth routes if the evaporation frequencies are high with respect to collision frequencies.[5] The qualitative trend of the free energy surfaces based on average DFT free energies at the same conditions is quite similar to the DLPNO results, but in the case of three-component clusters there are a few more formation steps which yield a lower free energy (see Supporting Information).

Figure 12 shows the overall evaporation rates for MBTCA clusters at 273 K. In the case of bimolecular sulfuric acid-MBTCA clusters, the most stable cluster is 2M3A with a total evaporation rate of 5 s^{-1}. The evaporation rates of other clusters are 2−10 orders of magnitude higher. The presence of bisulfate increases the evaporation rates of the three-component clusters. Similarly to the case of pinic acid, this is due to the strong interaction between sulfuric acid and bisulfate, meaning that all MBTCA−sulfuric acid−bisulfate clusters are evaporating fast toward the very stable 1A1B or 2A1B clusters. When there is no sulfuric acid, MBTCA and bisulfate are able to form a 1M1B cluster which is stable against evaporation, but the 2M1B cluster is unstable. The presence of ammonia can either increase or decrease the evaporation rates by several orders of magnitude. The most stable cluster is 3M2A1N, with an evaporation rate of 0.2 s^{-1}, which is 5 orders of magnitude lower than the corresponding bimolecular 3M2A cluster. Also ammonium can either increase or decrease the total evaporation rates by several orders of magnitude. The two-component MBTCA-ammonium clusters are particularly stable against evaporation. The total evaporation rates are reduced approximative 2 orders of magnitude when the temperature is decreased to 243 K (see Supporting

DOI: 10.1021/acs.jpca.7b03981
J. Phys. Chem. A 2017, 121, 4812−4824

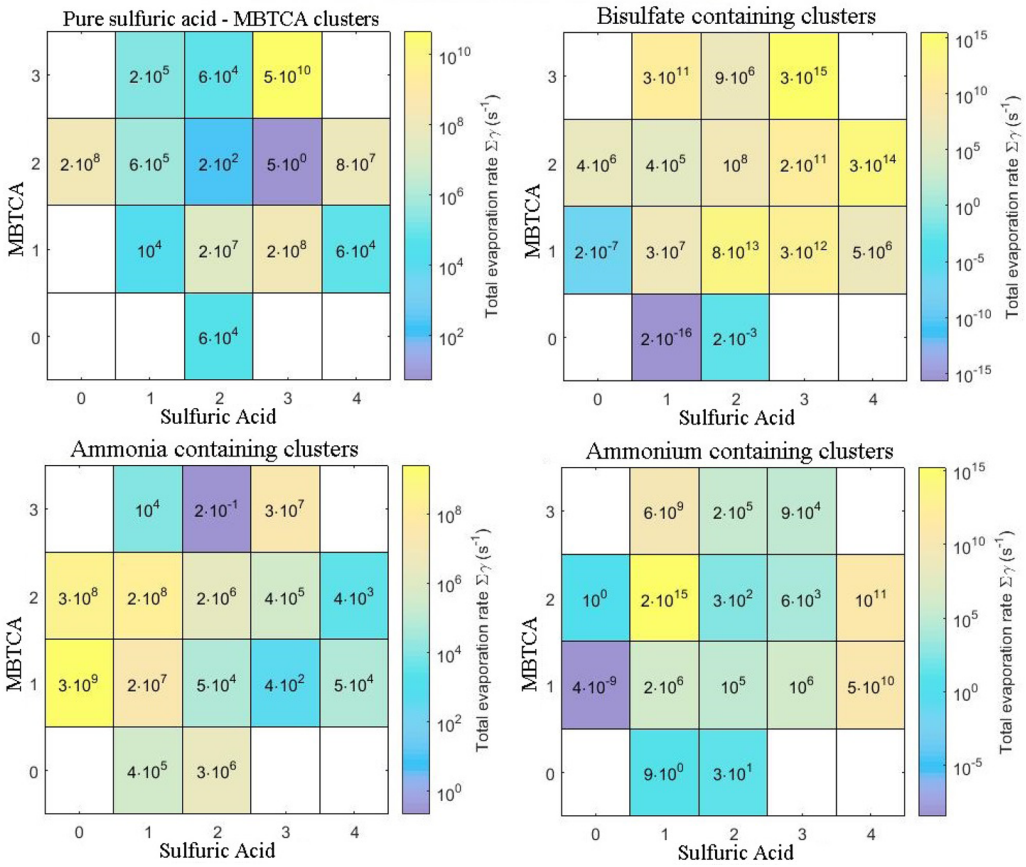

Figure 12. Overall evaporation rates ($\sum\gamma$ (s^{-1})) for MBTCA clusters at 273 K based on DLPNO//DFT free energies. Note the different color scale of the total evaporation rates.

Information), indicating that even at a low temperature only a few of the MBTCA clusters are stable against evaporation. We have also calculated the overall evaporation rates at 298 K, and the results indicate that none of the three-component clusters are stable against evaporation at a higher atmospheric temperature (see Supporting Information). For a lower-bound estimate for the evaporation rates, we have calculated the overall evaporation rates at 273 K based on the average DFT Gibbs free energies (see Supporting Information). The qualitative prediction of DFT is similar to that of DLPNO, with approximately 3 orders of magnitude lower evaporation rates. The results imply that there are only a few MBTCA clusters which are stable against evaporation at 273 K.

Most of the MBTCA–sulfuric acid–bisulfate clusters have several orders of magnitude higher total evaporation rates compared to the two-component MBTCA–sulfuric acid clusters. This is due to the very high stability of sulfuric acid–bisulfate clusters. For instance, the evaporation pathways for 1M1A1B clusters are

$$\text{1M1A1B} \rightarrow \text{1M1B} + \text{1A} \quad \gamma_{10} = 3 \times 10^{-2}\ \text{s}^{-1} \qquad \text{(R10)}$$

$$\text{1M1A1B} \rightarrow \text{1A1B} + \text{1M} \quad \gamma_{11} = 3 \times 10^{7}\ \text{s}^{-1} \qquad \text{(R11)}$$

$$\text{1M1A1B} \rightarrow \text{1M1A} + \text{1B} \quad \gamma_{12} = 1 \times 10^{-13}\ \text{s}^{-1} \qquad \text{(R12)}$$

indicating that the R11 is the rate-determining evaporation route.

The most stable ammonia-containing cluster is 3M2A1N, and the main evaporation routes for it are the monomer evaporations

$$\text{3M2A1N} \rightarrow \text{3M1A1N} + \text{1A} \quad \gamma_{13} = 1 \times 10^{-4}\ \text{s}^{-1} \qquad \text{(R13)}$$

$$\text{3M2A1N} \rightarrow \text{2M2A1N} + \text{1M} \quad \gamma_{14} = 5 \times 10^{-3}\ \text{s}^{-1} \qquad \text{(R14)}$$

$$\text{3M2A1N} \rightarrow \text{3M2A} + \text{1N} \quad \gamma_{15} = 2 \times 10^{-1}\ \text{s}^{-1} \qquad \text{(R15)}$$

where the evaporation of ammonia has the largest evaporation rate and thus it determines the total evaporation rate of 3M2A1N.

The very low stability of the 2M1A1C cluster can be explained by the very rapid evaporation of sulfuric acid monomer, with an evaporation rate of 2×10^{15} s^{-1}. The 3M3A1C cluster has a much lower overall evaporation rate than the corresponding 3M3A cluster. The main evaporation routes for the 3M3A1C cluster are

$$\text{3M3A1C} \rightarrow \text{3M2A1C} + \text{1A} \quad \gamma_{16} = 2 \times 10^{3}\ \text{s}^{-1} \qquad \text{(R16)}$$

$$\text{3M3A1C} \rightarrow \text{2M3A1C} + \text{1M} \quad \gamma_{17} = 7 \times 10^{4}\ \text{s}^{-1} \qquad \text{(R17)}$$

$$\text{3M3A1C} \rightarrow \text{2M2A1C} + \text{1M1A} \quad \gamma_{18} = 1 \times 10^{4}\ \text{s}^{-1} \qquad \text{(R18)}$$

$$\text{3M3A1C} \rightarrow \text{1M1C} + \text{2M3A} \quad \gamma_{19} = 1 \times 10^{3}\ \text{s}^{-1} \qquad \text{(R19)}$$

DOI: 10.1021/acs.jpca.7b03981
J. Phys. Chem. A 2017, 121, 4812–4824

whereas the MBTCA monomer evaporates from the 3M3A cluster with an evaporation rate of 5×10^{10} s^{-1}. This means that the presence of ammonium stabilizes the three MBTCA and three sulfuric acid containing clusters by 6 orders of magnitude with respect to evaporation. However, the evaporation rate of this cluster is still high, and thus it is likely that the 3M3A1C cluster would, in atmospheric conditions, evaporate rapidly instead of growing further.

It must be noted that the studied ammonia or ammonium containing clusters contain only one ammonia molecule (or cation). Especially in case of positively charged clusters, the most stable compositions may contain more ammonia molecules, possibly starting already from the first growth step which may be the formation of the relatively stable (NH_4^+)-(NH_3) dimer.[5] However, given the instability of the studied clusters, it does not seem likely that additional NH_3 molecules would be able to stabilize the three-component clusters against evaporation in atmospheric conditions.

4. CONCLUSIONS

We have investigated the effect of bisulfate, ammonia, and ammonium on the clustering of organic multicarboxylic acids and sulfuric acid. Both bisulfate and ammonium ions enhance the initial steps of cluster formation since the interaction with ions and sulfuric acid or carboxylic acid group is very strong. According to the Gibbs free energy surfaces at ambient concentrations, bisulfate stimulates growth along the sulfuric acid coordinate, whereas ammonium stimulates the growth along the organic acid coordinate. At atmospheric conditions and realistic vapor concentrations, however, it seems unlikely that the clusters can grow into larger stable clusters via the studied compounds. For electrically neutral clusters thermodynamically favorable growth direction was not identified. The most stable three-component cluster is found to consist of one ammonia, three MBTCA, and two sulfuric acid molecules. If this cluster is able to form, it could act as a seed for addition of other stabilizing vapor compounds. However, it does not seem probable that organic acids and sulfuric acid even together with bisulfate, ammonia, or ammonium can drive the observed new-particle formation events via clustering mechanisms. Investigation of the effect of adding multiple ammonia molecules would be an interesting topic for a future study to confirm this hypothesis, given the high abundance of ammonia in the atmospheric gas phase.

Since quantum chemical studies together with kinetic calculations have shown that α-pinene oxidation products cannot form clusters which are stable against evaporation at atmospheric conditions, but experimental studies have found organic compounds to participate in the initial steps of new-particle formation[10,11] especially via ion-induced pathways,[15] some other compounds or mechanisms are needed to explain observed formation events. One possible reason for the disagreement between experimental and theoretical findings might be the formation of covalently bound dimers or higher-order oligomers from monoterpene oxidation products[57−60] as well as the formation of organosulfates from sulfuric acid and oxidized organic compounds.[61] The multitude of proposed dimer formation reactions and molecular structures highlight both the complexity of the systems, and the large gap in the current knowledge.[62−64]

If dimer formation occurs via a condensation reaction (the addition and subsequent elimination reaction between closed-shell molecules), a catalyzing compound might be needed. This is because bimolecular condensation reactions are very unlikely in the gas phase due to the high activation energy barriers.[65−68] This implies that the covalently bound dimer or oligomer formation reactions could be occurring in the cluster, where other compounds, such as sulfuric acid, bases, or water, could act as the catalyst. Furthermore, if condensation reactions can take place in the cluster, the formed covalently bound dimer very likely has a lower vapor pressure than the monomers because of a higher molecular mass and a larger number of functional groups.[14,57] Hence the clusters in which real chemical reactions are occurring would be more stable against evaporation, and thus cluster-phase reactions might play a significant role in new-particle formation. Therefore, in addition to noncovalent interactions, chemical reactions should be also taken into consideration when studying cluster formation involving oxidized organic compounds.

■ ASSOCIATED CONTENT

Supporting Information

This material is available free of charge via the Internet at http://pubs.acs.org/. The Supporting Information is available free of charge on the ACS Publications website at DOI: 10.1021/acs.jpca.7b03981.

Mean absolute errors in the thermal contribution to the Gibbs free energy and relative computational times using the M06-2X functional with different basis sets, DLPNO−CCSD(T) binding energies as a function of basis set cardinal number, mean absolute errors in the binding energies and relative computational times using the DLPNO−CCSD(T) method and different basis sets, DLPNO−CCSD(T)/def2-QZVPP binding energies of MBTCA-sulfuric acid clusters with different local trafo types, actual Gibbs free energy surfaces of pinic acid and MBTCA clusters, based on the average DFT free energies at 273 K, $[H_2SO_4] = 10^7$ molecules/cm^3, and [pinic acid] = 10 ppt or [MBTCA] = 10 ppt, overall evaporation rates based on average DFT free energies for pinic acid and MBTCA clusters at 273 K, overall evaporation rates based on DLPNO//DFT free energies for pinic acid and MBTCA clusters at 243 K, and overall evaporation rates based on DLPNO//DFT free energies for pinic acid and MBTCA clusters at 298 K.(PDF)

■ AUTHOR INFORMATION

Corresponding Author

*E-mail: jonas.elm@helsinki.fi. Telephone: +45 28938085.

ORCID

Theo Kurtén: 0000-0002-6416-4931

Ilona Riipinen: 0000-0001-9085-2319

Jonas Elm: 0000-0003-3736-4329

Notes

The authors declare no competing financial interest.

■ ACKNOWLEDGMENTS

We thank the Academy of Finland, ERC Projects 257360-MOCAPAF and 692891-DAMOCLES, and Swedish Research Council Formas Project 2015-749 for funding, and the CSC-IT Center for Science in Espoo, Finland, for computational resources. N.M. thanks the Doctoral Program in Atmospheric Sciences (ATM-DP) for financial support. J.E. thanks the Carlsberg foundation for financial support.

DOI: 10.1021/acs.jpca.7b03981
J. Phys. Chem. A 2017, 121, 4812−4824

REFERENCES

(1) Kulmala, M.; Kontkanen, J.; Junninen, H.; Lehtipalo, K.; Manninen, H. E.; Nieminen, T.; Petäjä, T.; Sipilä, M.; Schobesberger, S.; Rantala, P.; et al. Direct Observations of Atmospheric Aerosol Nucleation. *Science* **2013**, *339*, 943−946.

(2) Zhang, R.; Khalizov, A.; Wang, L.; Hu, M.; Xu, W. Nucleation and Growth of Nanoparticles in the Atmosphere. *Chem. Rev.* **2012**, *112*, 1957−2011.

(3) Stevens, B.; Feingold, G. Untangling Aerosol Effects on Clouds and Precipitation in a Buffered System. *Nature* **2009**, *461*, 607−613.

(4) Husar, D. E.; Temelso, B.; Ashworth, A. L.; Shields, G. C. Hydration of the Bisulfate Ion: Atmospheric Implications. *J. Phys. Chem. A* **2012**, *116*, 5151−5163.

(5) Olenius, T.; Kupiainen-Määttä, O.; Ortega, I. K.; Kurtén, T.; Vehkamäki, H. Free Energy Barrier in the Growth of Sulfuric Acid - Ammonia and Sulfuric Acid - Dimethylamine Clusters. *J. Chem. Phys.* **2013**, *139*, 084312.

(6) Kurtén, T.; Torpo, L.; Ding, C.-G.; Vehkamäki, H.; Sundberg, M. R.; Laasonen, K.; Kulmala, M. A Density Functional Study on Water-Sulfuric Acid-Ammonia Clusters and Implications for Atmospheric Cluster Formation. *J. Geophys. Res.* **2007**, *112*, D04210.

(7) Loukonen, V.; Kurtén, T.; Ortega, I. K.; Vehkamäki, H.; Pádua, A. A. H.; Sellegri, K.; Kulmala, M. Enhancing Effect of Dimethylamine in Sulfuric Acid Nucleation in the Presence of Water - A Computational Study. *Atmos. Chem. Phys.* **2010**, *10*, 4961−4974.

(8) Schobesberger, S.; Junninen, H.; Bianchi, F.; Lönn, G.; Ehn, M.; Lehtipalo, K.; Dommen, J.; Ehrhart, S.; Ortega, I. K.; Franchin, A.; et al. Molecular Understanding of Atmospheric Particle Formation from Sulfuric Acid and Large Oxidized Organic Molecules. *Proc. Natl. Acad. Sci. U. S. A.* **2013**, *110*, 17223−17228.

(9) Kulmala, M.; Riipinen, I.; Sipilä, M.; Manninen, H. E.; Petäjä, T.; Junninen, H.; Maso, M. D.; Mordas, G.; Mirme, A.; Vana, M.; et al. Toward Direct Measurement of Atmospheric Nucleation. *Science* **2007**, *318*, 89−92.

(10) Ehn, M.; Thornton, J. A.; Kleist, E.; Sipilae, M.; Junninen, H.; Pullinen, I.; Springer, M.; Rubach, F.; Tillmann, R.; Lee, B.; et al. A Large Source of Low-Volatility Secondary Organic Aerosol. *Nature* **2014**, *506*, 476−479.

(11) Riccobono, F.; Schobesberger, S.; Scott, C. E.; Dommen, J.; Ortega, I. K.; Rondo, L.; Almeida, J.; Amorim, A.; Bianchi, F.; Breitenlechner, M.; et al. Oxidation Products of Biogenic Emissions Contribute to Nucleation of Atmospheric Particles. *Science* **2014**, *344*, 717−721.

(12) Elm, J.; Myllys, N.; Hyttinen, N.; Kurtén, T. Computational Study of the Clustering of a Cyclohexene Autoxidation Product $C_6H_8O_7$ with Itself and Sulfuric Acid. *J. Phys. Chem. A* **2015**, *119*, 8414−8421.

(13) Elm, J.; Myllys, N.; Luy, J.-N.; Kurtén, T.; Vehkamäki, H. The Effect of Water and Bases on the Clustering of a Cyclohexene Autoxidation Product $C_6H_8O_7$ with Sulfuric Acid. *J. Phys. Chem. A* **2016**, *120*, 2240−2249.

(14) Kurtén, T.; Tiusanen, K.; Roldin, P.; Rissanen, M.; Luy, J.-N.; Boy, M.; Ehn, M.; Donahue, N. α-pinene Autoxidation Products May Not Have Extremely Low Saturation Vapor Pressures Despite High O:C Ratios. *J. Phys. Chem. A* **2016**, *120*, 2569−2582.

(15) Kirkby, J.; Duplissy, J.; Sengupta, K.; Frege, C.; Gordon, H.; Williamson, C.; Heinritzi, M.; Simon, M.; Yan, C.; Almeida, J.; et al. Ion-induced Nucleation of Pure Biogenic Particles. *Nature* **2016**, *533*, 521−526.

(16) Seinfeld, J. H.; Pankow, J. F. Organic Atmospheric Particulate Material. *Annu. Rev. Phys. Chem.* **2003**, *54*, 121−140.

(17) Berndt, T.; Richters, S.; Kaethner, R.; Voigtländer, J.; Stratmann, F.; Sipilä, M.; Kulmala, M.; Herrmann, H. Gas-Phase Ozonolysis of Cycloalkenes: Formation ofHighly Oxidized RO2 Radicals and Their Reactions with NO, NO2, SO2, and Other RO2 Radicals. *J. Phys. Chem. A* **2015**, *119*, 10336−10348.

(18) Crounse, J. D.; Nielsen, L. B.; Jørgensen, S.; Kjaergaard, H. G.; Wennberg, P. O. Autoxidation of Organic Compounds in the Atmosphere. *J. Phys. Chem. Lett.* **2013**, *4*, 3513−3520.

(19) Jokinen, T.; Sipilä, M.; Richters, S.; Kerminen, V.-M.; Paasonen, P.; Stratmann, F.; Worsnop, D.; Kulmala, M.; Ehn, M.; Herrmann, H.; et al. Rapid Autoxidation Forms Highly Oxidized RO2 Radicals in the Atmosphere. *Angew. Chem., Int. Ed.* **2014**, *53*, 14596−14600.

(20) Kurtén, T.; Rissanen, M. P.; Mackeprang, K.; Thornton, J. A.; Hyttinen, N.; Jørgensen, S.; Ehn, M.; Kjaergaard, H. G. Computational Study of Hydrogen Shifts and Ring-Opening Mechanisms in α-pinene Ozonolysis Products. *J. Phys. Chem. A* **2015**, *119*, 11366−11375.

(21) Hoffmann, T.; Bandur, R.; Marggraf, U.; Linscheid, M. Molecular Composition of Organic Aerosols Formed in the α-pinene/O3 Reaction: Implications for New Particle Formation Processes. *J. Geophys. Res. Atmos.* **1998**, *103*, 25569−25578.

(22) Christoffersen, T.; Hjorth, J.; Horie, O.; Jensen, N.; Kotzias, D.; Molander, L.; Neeb, P.; Ruppert, L.; Winterhalter, R.; Virkkula, A.; et al. Cis-pinic Acid, a Possible Precursor for Organic Aerosol Formation from Ozonolysis of α-pinene. *Atmos. Environ.* **1998**, *32*, 1657−1661.

(23) Szmigielski, R.; Surratt, J. D.; Gómez-González, Y.; Van der Veken, P.; Kourtchev, I.; Vermeylen, R.; Blockhuys, F.; Jaoui, M.; Kleindienst, T. E.; Lewandowski, M. 3-methyl-1,2,3-butanetricarboxylic Acid: An Atmospheric Tracer for Terpene Secondary Organic Aerosol. *Geophys. Res. Lett.* **2007**, *34*, L24811 DOI: 10.1029/2007GL031338.

(24) Elm, J.; Myllys, N.; Olenius, T.; Halonen, R.; Kurtén, T.; Vehkamaki, H. Formation of Atmospheric Molecular Clusters Consisting of Sulfuric Acid and $C_8H_{12}O_6$ Tricarboxylic Acid. *Phys. Chem. Chem. Phys.* **2017**, *19*, 4877−4886.

(25) Elm, J.; Kurtén, T.; Bilde, M.; Mikkelsen, K. V. Molecular Interaction of Pinic Acid with Sulfuric Acid: Exploring the Thermodynamic Landscape of Cluster Growth. *J. Phys. Chem. A* **2014**, *118*, 7892−7900.

(26) Svensmark, H.; Friis-Christensen, E. Variation of Cosmic Ray Flux and Global Cloud Coverage - A Missing Link in Solar-climate Relationships. *J. Atmos. Sol.-Terr. Phys.* **1997**, *59*, 1225−1232.

(27) Carslaw, K. S.; Harrison, R. G.; Kirkby, J. Cosmic Rays, Clouds, and Climate. *Science* **2002**, *298*, 1732−1737.

(28) Yu, F.; Turco, R. P. Ultrafine Aerosol Formation Via Ion-Mediated Nucleation. *Geophys. Res. Lett.* **2000**, *27*, 883−886.

(29) Paciga, A. L.; Riipinen, I.; Pandis, S. N. Effect of Ammonia on the Volatility of Organic Diacids. *Environ. Sci. Technol.* **2014**, *48*, 13769−13775.

(30) Scott, W.; Cattell, F. Vapor Pressure of Ammonium Sulfates. *Atmos. Environ.* **1979**, *13*, 307−317.

(31) Yli-Juuti, T.; Zardini, A. A.; Eriksson, A. C.; Hansen, A. M. K.; Pagels, J. H.; Swietlicki, E.; Svenningsson, B.; Glasius, M.; Worsnop, D. R.; Riipinen, I.; et al. Volatility of Organic Aerosol: Evaporation of Ammonium Sulfate/Succinic Acid Aqueous Solution Droplets. *Environ. Sci. Technol.* **2013**, *47*, 12123−12130.

(32) Häkkinen, S. A. K.; McNeill, V. F.; Riipinen, I. Effect of Inorganic Salts on the Volatility of Organic Acids. *Environ. Sci. Technol.* **2014**, *48*, 13718−13726.

(33) Elm, J.; Bilde, M.; Mikkelsen, K. V. Influence of Nucleation Precursors on the Reaction Kinetics ofMethanol with the OH Radical. *J. Phys. Chem. A* **2013**, *117*, 6695−6701.

(34) Elm, J.; Fard, M.; Bilde, M.; Mikkelsen, K. V. Interaction of Glycine with Common Atmospheric Nucleation Precursors. *J. Phys. Chem. A* **2013**, *117*, 12990−12997.

(35) Myllys, N.; Elm, J.; Kurtén, T. Density Functional Theory Basis Set Convergence of Sulfuric Acid-containing Molecular Clusters. *Comput. Theor. Chem.* **2016**, *1098*, 1−12.

(36) Ortega, I. K.; Kurtén, T.; Vehkamäki, H.; Kulmala, M. The Role of Ammonia in Sulfuric Acid Ion Induced Nucleation. *Atmos. Chem. Phys.* **2008**, *8*, 2859−2867.

(37) Myllys, N.; Elm, J.; Halonen, R.; Kurtén, T.; Vehkamäki, H. Coupled Cluster Evaluation of the Stability of Atmospheric Acid - Base Clusters with up to 10 Molecules. *J. Phys. Chem. A* **2016**, *120*, 621−630.

(38) Zhao, Y.; Truhlar, D. G. The M06 Suite of Density Functionals for Main Group Thermochemistry, Thermochemical Kinetics, Non-

DOI: 10.1021/acs.jpca.7b03981
J. Phys. Chem. A 2017, 121, 4812−4824

covalent Interactions, Excited States, and Transition Elements: Two New Functionals and Systematic Testing of Four M06-class Functionals and 12 Other Functionals. *Theor. Chem. Acc.* **2008**, *120*, 215−241.
(39) Perdew, J. P.; Wang, Y. Accurate and Simple Analytic Representation of the Electron-gas Correlation Energy. *Phys. Rev. B: Condens. Matter Mater. Phys.* **1992**, *45*, 13244−13249.
(40) Chai, J.-D.; Head-Gordon, M. Long-range Corrected Hybrid Density Functionals with Damped Atom-atom Dispersion Corrections. *Phys. Chem. Chem. Phys.* **2008**, *10*, 6615−6620.
(41) Krishnan, R.; Binkley, J. S.; Seeger, R.; Pople, J. A. Self-consistent Molecular Orbital Methods. XX. A Basis Set for Correlated Wave Functions. *J. Chem. Phys.* **1980**, *72*, 650−654.
(42) Elm, J.; Bilde, M.; Mikkelsen, K. V. Assessment of Binding Energies of Atmospherically Relevant Clusters. *Phys. Chem. Chem. Phys.* **2013**, *15*, 16442−16445.
(43) Elm, J.; Bilde, M.; Mikkelsen, K. V. Assessment of Density Functional Theory in Predicting Structures and Free Energies of Reaction of Atmospheric Prenucleation Clusters. *J. Chem. Theory Comput.* **2012**, *8*, 2071−2077.
(44) Leverentz, H. R.; Siepmann, J. I.; Truhlar, D. G.; Loukonen, V.; Vehkamäki, H. Energetics of Atmospherically Implicated Clusters Made of Sulfuric Acid, Ammonia, and Dimethyl Amine. *J. Phys. Chem. A* **2013**, *117*, 3819−3825.
(45) Temelso, B.; Archer, K. A.; Shields, G. C. Benchmark Structures and Binding Energies of Small Water Clusters with Anharmonicity Corrections. *J. Phys. Chem. A* **2011**, *115*, 12034−12046.
(46) Grimme, S. Supramolecular Binding Thermodynamics by Dispersion-corrected Density Functional Theory. *Chem. - Eur. J.* **2012**, *18*, 9955−9964.
(47) Frisch, M. J.; Trucks, G. W.; Schlegel, H. B.; Scuseria, G. E.; Robb, M. A.; Cheeseman, J. R.; Scalmani, G.; Barone, V.; Mennucci, B.; Petersson, G. A. et al. *Gaussian09*, Revision D.01; Gaussian Inc.: Wallingford, CT, 2009.
(48) Riplinger, C.; Neese, F. An Efficient and Near Linear Scaling Pair Natural Orbital Based Local Coupled Cluster Method. *J. Chem. Phys.* **2013**, *138*, 034106.
(49) Riplinger, C.; Sandhoefer, B.; Hansen, A.; Neese, F. Natural Triple Excitations in Local Coupled Cluster Calculations with Pair Natural Orbitals. *J. Chem. Phys.* **2013**, *139*, 134101.
(50) Weigend, F.; Ahlrichs, R. Balanced Basis Sets of Split Valence, Triple Zeta Valence and Quadruple Zeta Valence Quality for H To Rn: Design and Assessment of Accuracy. *Phys. Chem. Chem. Phys.* **2005**, *7*, 3297−3305.
(51) Neese, F. The ORCA Program System. *Wiley Interdiscip. Rev. Comput. Mol. Sci.* **2012**, *2*, 73−78.
(52) Chapman, S.; Cowling, T. G. *The mathematical theory of non-uniform gases*; University Press: Cambridge, U.K., 1970.
(53) Kupiainen-Määttä, O.; Olenius, T.; Kurtén, T.; Vehkamäki, H. CIMS Sulfuric Acid Detection Efficiency Enhanced by Amines Due to Higher Dipole Moments: A Computational Study. *J. Phys. Chem. A* **2013**, *117*, 14109−14119.
(54) Su, T.; Chesnavich, W. J. Parametrization of the Ion - Polar Molecule Collision Rate Constant by Trajectory Calculations. *J. Chem. Phys.* **1982**, *76*, 5183−5185.
(55) Ortega, I. K.; Kupiainen, O.; Kurtén, T.; Olenius, T.; Wilkman, O.; McGrath, M. J.; Loukonen, V.; Vehkamäki, H. From Quantum Chemical Formation Free Energies to Evaporation Rates. *Atmos. Chem. Phys.* **2012**, *12*, 225−235.
(56) Elm, J.; Myllys, N.; Kurtén, T. Phosphoric Acid - A Potentially Elusive Participant in Atmospheric New Particle Formation. *Mol. Phys.* **2016**, 1−12.
(57) Mohr, C.; Lopez-Hilfiker, F. D.; Yli-Juuti, T.; Heitto, A.; Lutz, A.; Hallquist, M.; D'Ambro, E. L.; Rissanen, M. P.; Hao, L.; Schobesberger, S. Ambient Observations of Dimers from Terpene Oxidation in the Gas Phase: Implications for New Particle Formation and Growth. *Geophys. Res. Lett.* **2017**, *44*, 2958.
(58) Kourtchev, I.; Giorio, C.; Manninen, A.; Wilson, E.; Mahon, B.; Aalto, J.; Kajos, M.; Venables, D.; Ruuskanen, T.; Levula, J.; et al. Enhanced Volatile Organic Compounds Emissions and Organic Aerosol Mass Increase the Oligomer Content of Atmospheric Aerosols. *Sci. Rep.* **2016**, *6*, 35038.
(59) Camredon, M.; Hamilton, J. F.; Alam, M. S.; Wyche, K. P.; Carr, T.; White, I. R.; Monks, P. S.; Rickard, A. R.; Bloss, W. J. Distribution of Gaseous and Particulate Organic Composition During Dark α-pinene Ozonolysis. *Atmos. Chem. Phys.* **2010**, *10*, 2893−2917.
(60) Yasmeen, F.; Vermeylen, R.; Szmigielski, R.; Iinuma, Y.; Böge, O.; Herrmann, H.; Maenhaut, W.; Claeys, M. Terpenylic Acid and Related Compounds: Precursors for Dimers in Secondary Organic Aerosol from the Ozonolysis of α- and β-pinene. *Atmos. Chem. Phys.* **2010**, *10*, 9383−9392.
(61) Surratt, J. D.; Kroll, J. H.; Kleindienst, T. E.; Edney, E. O.; Claeys, M.; Sorooshian, A.; Ng, N. L.; Offenberg, J. H.; Lewandowski, M.; Jaoui, M.; et al. Evidence for Organosulfates in Secondary Organic Aerosol. *Environ. Sci. Technol.* **2007**, *41*, 517−527.
(62) Kristensen, K.; Cui, T.; Zhang, H.; Gold, A.; Glasius, M.; Surratt, J. D. Dimers in α-pinene Secondary Organic Aerosol: Effect of Hydroxyl Radical, Ozone, Relative Humidity and Aerosol Acidity. *Atmos. Chem. Phys.* **2014**, *14*, 4201−4218.
(63) Zhang, X.; McVay, R. C.; Huang, D. D.; Dalleska, N. F.; Aumont, B.; Flagan, R. C.; Seinfeld, J. H. Formation and Evolution of Molecular Products in α-pinene Secondary Organic Aerosol. *Proc. Natl. Acad. Sci. U. S. A.* **2015**, *112*, 14168−14173.
(64) Kristensen, K.; Enggrob, K. L.; King, S. M.; Worton, D. R.; Platt, S. M.; Mortensen, R.; Rosenoern, T.; Surratt, J. D.; Bilde, M.; Goldstein, A. H.; et al. Formation and Occurrence of Dimer Esters of Pinene Oxidation Products in Atmospheric Aerosols. *Atmos. Chem. Phys.* **2013**, *13*, 3763−3776.
(65) Louie, M. K.; Francisco, J. S.; Verdicchio, M.; Klippenstein, S. J.; Sinha, A. Dimethylamine Addition to Formaldehyde Catalyzed by a Single Water Molecule: A Facile Route for Atmospheric Carbinolamine Formation and Potential Promoter of Aerosol Growth. *J. Phys. Chem. A* **2016**, *120*, 1358−1368.
(66) Duporté, G.; Riva, M.; Parshintsev, J.; Heikkinen, E.; Barreira, L. M.; Myllys, N.; Heikkinen, L.; Hartonen, K. M.; Kulmala, M.; Ehn, M. Chemical Characterization of Gas- and Particle-Phase Products from the Ozonolysis of α-pinene in the Presence of Dimethylamine. *Environ. Sci. Technol.* **2017**, *51*, 5602.
(67) Patil, M. P.; Sunoj, R. B. Insights on Co-Catalyst-Promoted Enamine Formation between Dimethylamine and Propanal through Ab Initio and Density Functional Theory Study. *J. Org. Chem.* **2007**, *72*, 8202−8215.
(68) Sunoj, R. B.; Anand, M. Microsolvated Transition State Models for Improved Insight Into Chemical Properties and Reaction Mechanisms. *Phys. Chem. Chem. Phys.* **2012**, *14*, 12715−12736.

DOI: 10.1021/acs.jpca.7b03981
J. Phys. Chem. A 2017, 121, 4812−4824